Supplementary Material:

Atheroma-specific lipids in *ldlr*$^{-/-}$ and *apoe*$^{-/-}$mice using 2D and 3D matrix-assisted laser desorption/ionization mass spectrometry imaging

Jianhua Cao, [1] Pieter Goossens, [2] Marta Martin-Lorenzo, [1] Frédéric Dewez, [1,3] Britt S. R. Claes,[1] Erik A. L. Biessen, [2] Ron M.A. Heeren,[1] and Benjamin Balluff [1]

[1] Maastricht Multimodal Molecular Imaging Institute (M4I), Maastricht University, Maastricht, The Netherlands

[2] Maastricht UMC+, Pathology Department, Cardiovascular Research Institute Maastricht (CARIM), Maastricht, The Netherlands

[3] Mass Spectrometry Laboratory (MSLab), University of Liège, Liège, Belgium

Supplementary Table 1. Plaque specific *m/z* species (n = 33) and corresponding correlation coefficients in the *ldlr*$^{-/-}$ mouse model.

Observed m/z by TOF	Pearson correlation coefficient *ldlr*$^{-/-}$	Observed *m/z* by Orbitrap	Lipid assignment	MS experiment level for ID	Ion mode	Mass error (in ppm)
409.3	0.47	409.2366	[LPA 16:0–H]$^-$	MS1	NEG	+1.3
435.3	0.50	435.2522	[LPA 18:1–H]$^-$	MS1	NEG	+1.1
436.3	0.42	436.2833	[LPE O-16:1–H]$^-$	MS1	NEG	+1.0
437.3	0.43	437.2679	[LPA 18:0-H]$^-$	MS1	NEG	+1.2
459.2	0.50	459.2476	[LPA 18:1+Na]$^+$	MS1	POS	-1.3
463.3	0.41	463.2839	[LPA 20:1–H]$^-$	MS1	NEG	+1.9
464.3	0.44	464.3142	[LPE O-18:1–H]$^-$	MS1	NEG	-1.0
470.9	0.59	/	/	/	POS	/
480.3	0.52	480.3099	[LPE 18:0–H]$^-$/ [LPC 16:0–CH_3]$^-$	MS2	NEG	+0.6
481.0	0.52	/	/	/	POS	/
482.3	0.55	482.3600	[LPC O-16:0+H]$^+$/ [LPE O-19:0+H]$^+$	MS1	POS	-1.0
487.3	0.47	487.2790	[LPA 20:1+Na]$^+$	MS1	POS	-1.0
496.3	0.58	496.3398	[LPC 16:0+H]$^+$	MS2	POS	+0.0
496.6	0.60	/	/	/	POS	/
498.7	0.55	/	/	/	POS	/
506.3	0.43	506.3257	[LPC 18:1-CH_3]$^-$/ [LPE 20:1-H]$^-$	MS1	NEG	+1.0
510.4	0.59	510.3554	[LPC 17:0+H]$^+$ / [LPE 20:0+H]$^+$	MS1	POS	+0.0
518.3	0.59	518.3216	[LPC 16:0+Na]$^+$	MS2	POS	-0.2
520.3	0.63	520.3400	[LPC 18:2+H]$^+$	MS2	POS	+0.4
522.4	0.56	522.3557	[LPC 18:1+H]$^+$	MS2	POS	+0.6
524.4	0.45	524.3717	[LPC 18:0+H]+	MS2	POS	+1.1
524.6	0.48	/	/	/	POS	/
534.3	0.57	534.2951	[LPC 16:0+K]$^+$	MS2	POS	-0.9
538.4	0.43	538.3862	[LPC 19:0+H]$^+$/ [LPE 22:0+H]$^+$	MS1	POS	-1.0
542.4	0.58	542.3213	[LPC 18:2+Na]$^+$	MS1	POS	-0.8
544.4	0.59	544.3389	[LPC 18:1+Na]$^+$	MS2	POS	+2.8
546.4	0.56	546.3540	[LPC 18:0+Na]$^+$	MS2	POS	+1.8
560.3	0.49	560.3123	[LPC 18:1+K]$^+$	MS2	POS	+0.0
562.3	0.49	562.3278	[LPC 18:0+K]$^+$	MS2	POS	+0.0
599.3	0.41	599.3216	[LPI 18:0–H]$^-$	MS2	NEG	+2.4
676.8	0.42	/	/	/	POS	/
689.6	0.42	689.5620	[SM d18:0_16:0-CH_3]$^-$	MS2	NEG	+0.7
727.6	0.40	727.5731	[SM 34:0;2+Na]$^+$	MS2	POS	+1.0

Supplementary Table 2. Plaque specific m/z species (n = 43) and corresponding correlation coefficients in the *apoe*$^{-/-}$ mouse model.

Observed m/z by TOF	Pearson correlation coefficient *apoe*$^{-/-}$	Observed *m/z* by Orbitrap	Lipid assignment	MS experiment level for ID	Ion mode	Mass error (in ppm)
409.3	0.61	409.2366	[LPA 16:0–H]$^-$	MS1	NEG	+1.3
459.2	0.46	459.2476	[LPA 18:1+Na]$^+$	MS1	POS	-1.3
463.3	0.54	463.2839	[LPA 20:1–H]$^-$	MS1	NEG	+1.9
464.3	0.59	464.3142	[LPE O-18:1–H]$^-$	MS1	NEG	-1.0
480.3	0.62	480.3099	[LPE 18:0–H]$^-$/ [LPC 16:0–CH_3]$^-$	MS2	NEG	+0.6
481.3	0.57	481.3000	/	/	NEG	/
482.3	0.50	482.3600	[LPC O-16:0+H]$^+$/ [LPE O-19:0+H]$^+$	MS1	POS	-1.0
487.3	0.44	487.2790	[LPA 20:1+Na]$^+$	MS1	POS	-1.0
496.3	0.62	496.3398	[LPC 16:0+H]$^+$	MS2	POS	+0.0
496.6	0.49	/	/	/	POS	/
506.3	0.41	506.3257	[LPC 18:1-CH_3]$^-$/ [LPE 20:1-H]$^-$	MS1	NEG	+1.0
508.3	0.58	508.3411	[LPC 18:0-CH_3]$^-$	MS2	NEG	+0.4
510.4	0.55	510.3554	[LPC 17:0+H]$^+$ / [LPE 20:0+H]$^+$	MS1	POS	+0.0
518.3	0.63	518.3216	[LPC 16:0+Na]$^+$	MS2	POS	-0.2
520.3	0.63	520.3400	[LPC 18:2+H]$^+$	MS2	POS	+0.4
522.4	0.59	522.3557	[LPC 18:1+H]$^+$	MS2	POS	+0.6
524.4	0.52	524.3717	[LPC 18:0+H]+	MS2	POS	+1.1
534.3	0.57	534.2951	[LPC 16:0+K]$^+$	MS2	POS	-0.9
538.4	0.53	538.3862	[LPC 19:0+H]$^+$/ [LPE 22:0+H]$^+$	MS1	POS	-1.0
542.4	0.57	542.3213	[LPC 18:2+Na]$^+$	MS1	POS	-0.8
544.4	0.57	544.3389	[LPC 18:1+Na]$^+$	MS2	POS	+2.8
546.4	0.49	546.3540	[LPC 18:0+Na]$^+$	MS2	POS	+1.8
560.3	0.45	560.3123	[LPC 18:1+K]$^+$	MS2	POS	+0.0
562.3	0.49	562.3278	[LPC 18:0+K]$^+$	MS2	POS	+0.0
574.5	0.57	574.4520	/	/	NEG	/
588.5	0.53	588.4678	/	/	NEG	/
590.4	0.48	590.4471	/	/	NEG	/
599.3	0.52	599.3216	[LPI 18:0–H]$^-$	MS2	NEG	+2.4
602.5	0.52	602.4836	/	/	NEG	/
604.5	0.54	604.4628	/	/	NEG	/
616.5	0.51	616.4722	[CerP 34:1;2–H]$^-$	MS1	NEG	+1.7
618.5	0.54	618.4877	[CerP 34:0;2–H]$^-$	MS1	NEG	+1.5
619.3	0.49	619.2895	[LPI 20:4-H]$^-$	MS2	NEG	+0.7
642.5	0.52	642.4881	[CerP 36:2;2-H]$^-$	MS1	NEG	+2.0
644.5	0.43	644.5038	[CerP 36:1;2-H]$^-$	MS1	NEG	+2.1
676.5	0.42	/	/	/	POS	/
687.6	0.52	687.5462	[SM d18:1_16:0-CH_3]$^-$	MS2	NEG	+2.2
689.6	0.53	689.5620	[SM d18:0_16:0-CH_3]$^-$	MS2	NEG	+0.7
727.6	0.44	727.5731	[SM 34:0;2+Na]$^+$	MS2	POS	+1.0

795.6	0.42	795.6404	/	/	NEG	/
796.6	0.41	796.6438	[ACer 50:6;4-H]$^-$	MS1	NEG	-2.8
797.6	0.47	797.6561	[CerPE 44:2;2-H]$^-$ /[EPC 44:2;2-H]$^-$	MS1	NEG	+2.4
799.7	0.43	799.6718	[CerPE 44:1;2-H]$^-$ /[EPC 44:1;2-H]$^-$	MS1	NEG	+2.4

Supplementary Table 3. Plaque specific m/z species (n = 22) and corresponding correlation coefficients in the 3D *apoe*$^{-/-}$ mouse.

Observed m/z by TOF	Lipid assignment	Pearson correlation coefficient
459.2	$[LPA\ 18:1+Na]^+$	0.55
463.3	$[LPA\ 20:1–H]^-$	0.48
464.3	$[LPE\ O\text{-}18:1–H]^-$	0.63
480.3	$[LPE\ 18:0–H]^-$/ $[LPC\ 16:0–CH_3]^-$	0.59
487.3	$[LPA\ 20:1+Na]^+$	0.54
496.3	$[LPC\ 16:0+H]^+$	0.53
496.6	/	0.53
510.4	$[LPC\ 17:0+H]^+$ / $[LPE\ 20:0+H]^+$	0.61
518.3	$[LPC\ 16:0+Na]^+$	0.64
520.3	$[LPC\ 18:2+H]^+$	0.60
522.4	$[LPC\ 18:1+H]^+$	0.61
524.4	[LPC 18:0+H]+	0.41
534.3	$[LPC\ 16:0+K]^+$	0.59
538.4	$[LPC\ 19:0+H]^+$/ $[LPE\ 22:0+H]^+$	0.58
542.4	$[LPC\ 18:2+Na]^+$	0.63
544.4	$[LPC\ 18:1+Na]^+$	0.60
546.4	$[LPC\ 18:0+Na]^+$	0.60
560.3	$[LPC\ 18:1+K]^+$	0.55
562.3	$[LPC\ 18:0+K]^+$	0.52
599.3	$[LPI\ 18:0–H]^-$	0.56
689.6	$[SM\ d18:0\_16:0\text{-}CH_3]^-$	0.56
727.6	$[SM\ 34:0;2+Na]^+$	0.58

Supplementary Fig. 1 Visualization of 10 plaque specific *m/z* species in found in 11 *ldlr*$^{-/-}$ mice in negative ion mode.

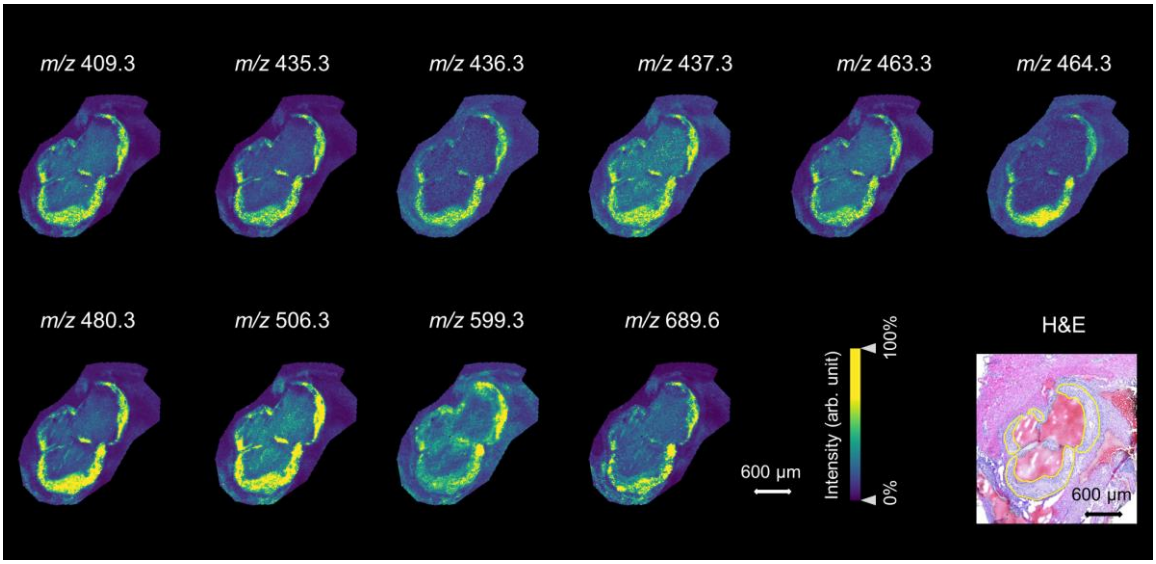

Supplementary Fig. 2 Visualization of 23 plaque specific *m/z* species found in 4 *ldlr*$^{-/-}$ mice in positive ion mode.

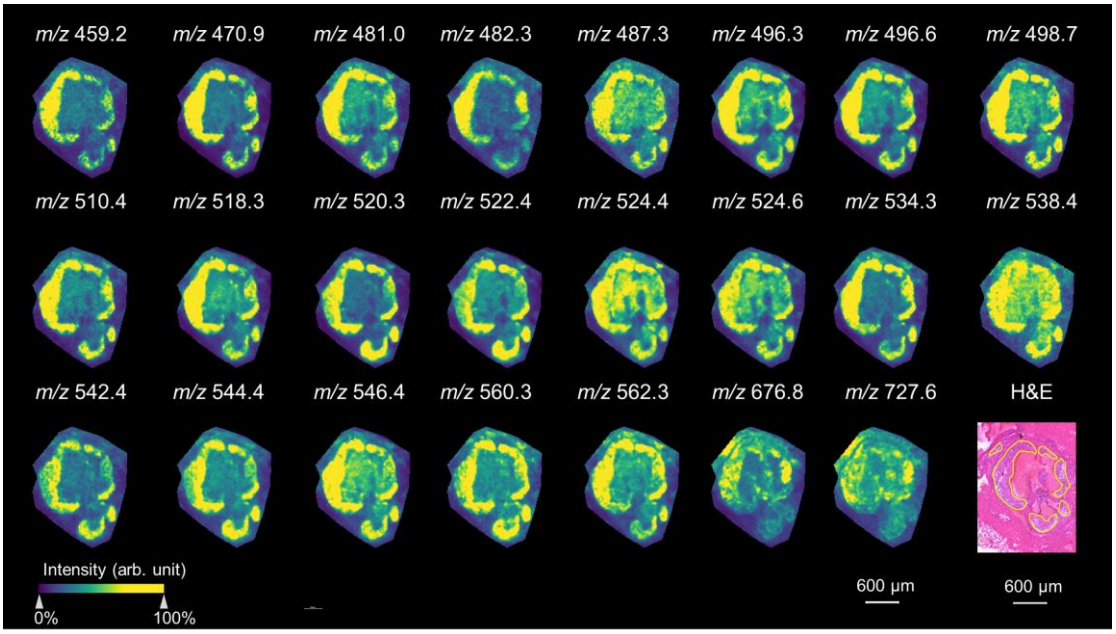

Supplementary Fig. 3 Visualization of 24 plaque specific *m/z* species found in 4 *apoe*$^{-/-}$ mice in negative ion mode.

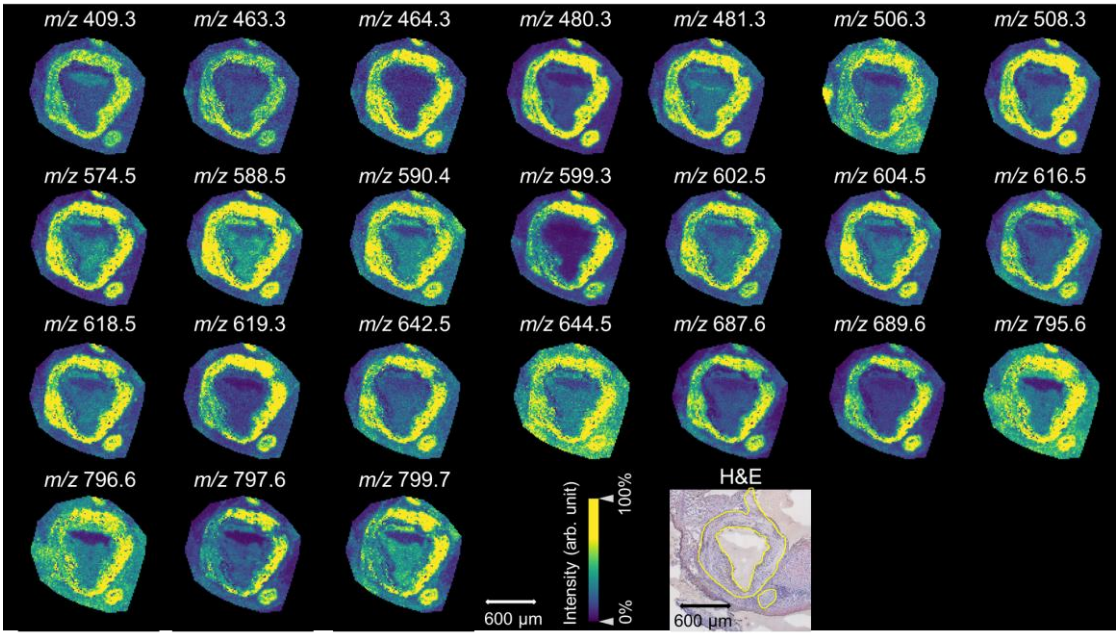

Supplementary Fig. 4 Visualization of 19 plaque specific *m/z* species found in 4 *apoe*$^{-/-}$ mice in positive ion mode.

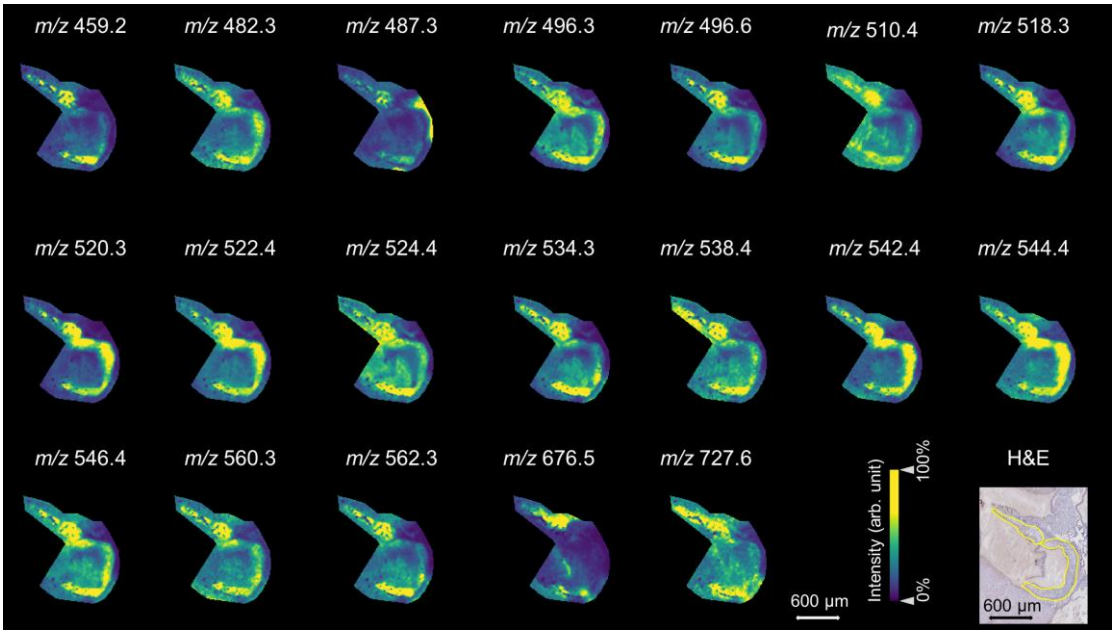

Supplementary Fig. 5 MS/MS spectrum of *m/z* 480.3099 ([LPE 18:0-H]$^-$ /[LPC 16:0-CH_3]$^-$)

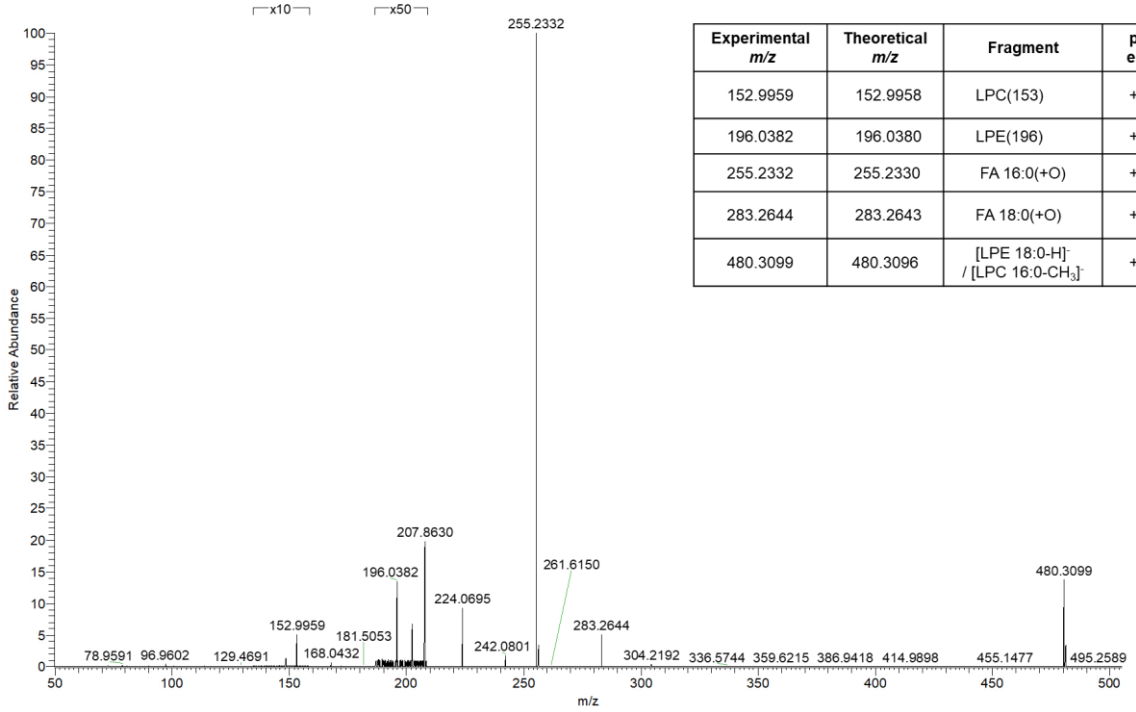

Experimental *m/z*	Theoretical *m/z*	Fragment	ppm error
152.9959	152.9958	LPC(153)	+0.7
196.0382	196.0380	LPE(196)	+1.0
255.2332	255.2330	FA 16:0(+O)	+0.8
283.2644	283.2643	FA 18:0(+O)	+0.4
480.3099	480.3096	[LPE 18:0-H]$^-$ / [LPC 16:0-CH_3]$^-$	+0.6

Supplementary Fig. 6 MS/MS spectrum of *m/z* 496.3398 ([LPC 16:0+H]$^+$)

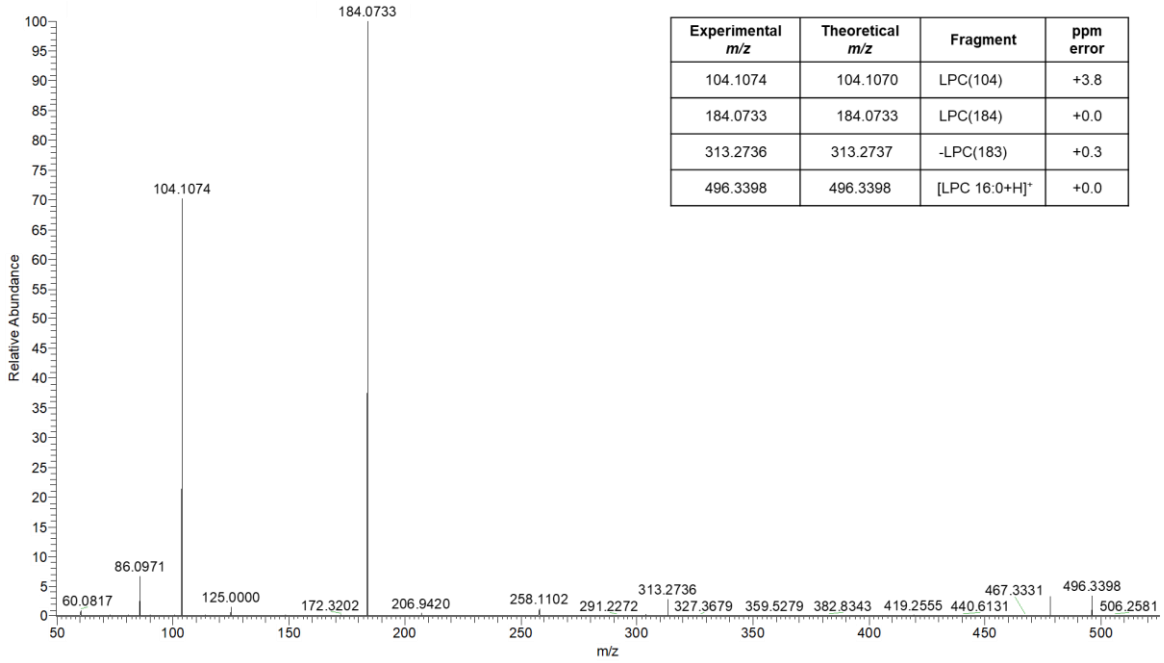

Experimental *m/z*	Theoretical *m/z*	Fragment	ppm error
104.1074	104.1070	LPC(104)	+3.8
184.0733	184.0733	LPC(184)	+0.0
313.2736	313.2737	-LPC(183)	+0.3
496.3398	496.3398	[LPC 16:0+H]$^+$	+0.0

Supplementary Fig. 7 MS/MS spectrum of m/z 508.3411 ([LPC 18:0-CH3]-)

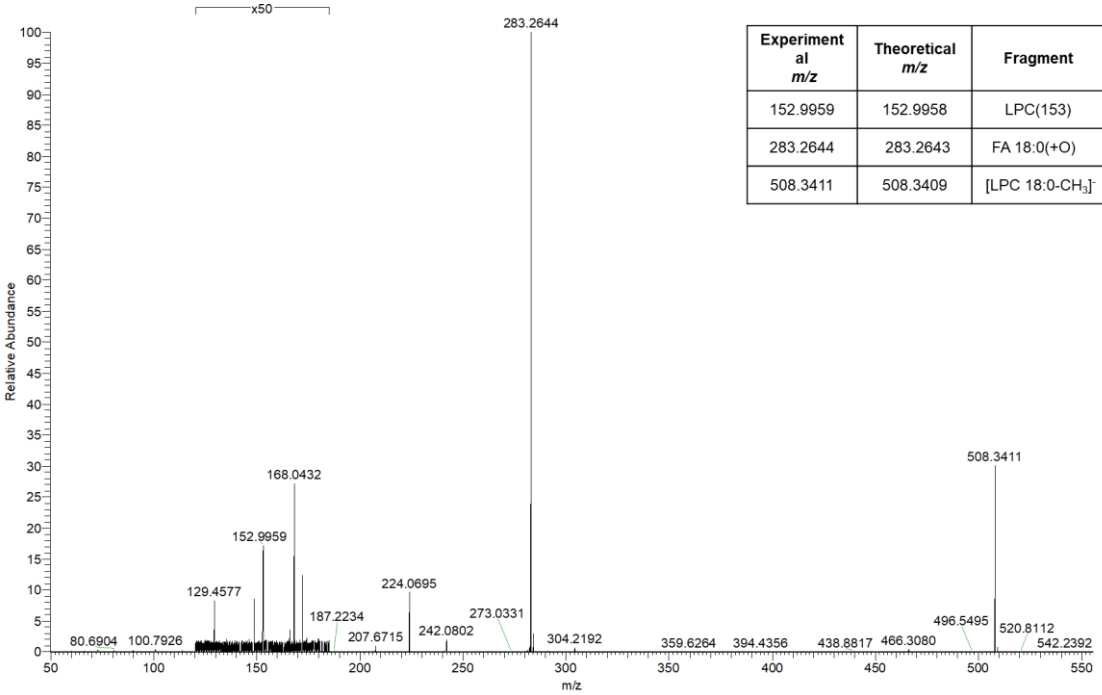

Experimental *m/z*	Theoretical *m/z*	Fragment	ppm error
152.9959	152.9958	LPC(153)	+0.7
283.2644	283.2643	FA 18:0(+O)	+0.4
508.3411	508.3409	$[LPC\ 18:0\text{-}CH_3]^-$	+0.4

Supplementary Fig. 8 MS/MS spectrum of m/z 518.3216 ([LPC 16:0+Na]+)

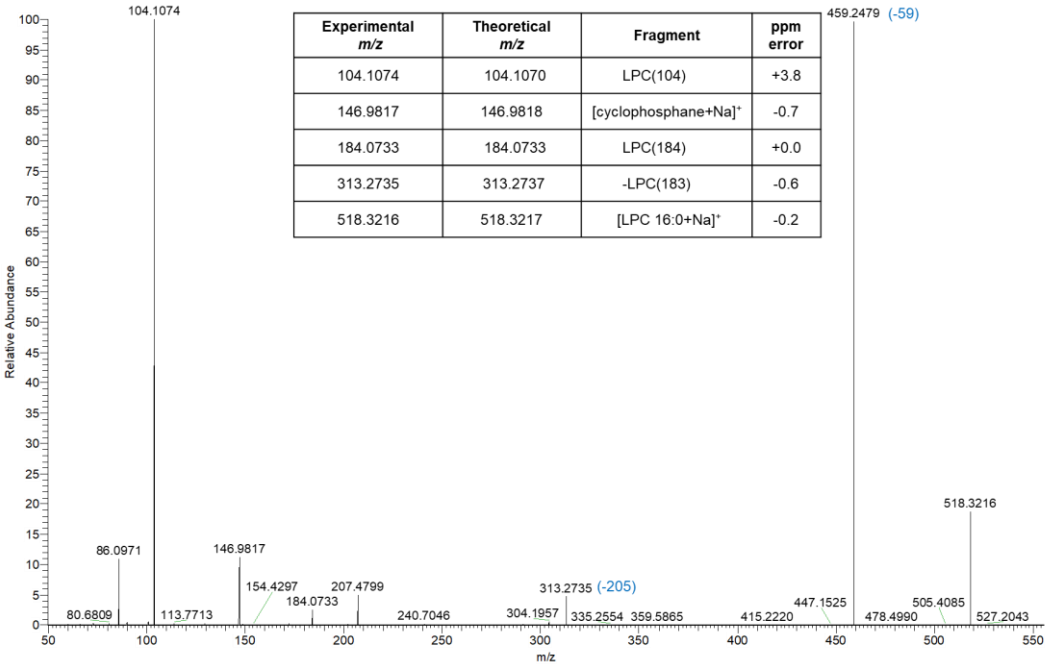

Experimental *m/z*	Theoretical *m/z*	Fragment	ppm error
104.1074	104.1070	LPC(104)	+3.8
146.9817	146.9818	[cyclophosphane+Na]$^+$	-0.7
184.0733	184.0733	LPC(184)	+0.0
313.2735	313.2737	-LPC(183)	-0.6
518.3216	518.3217	[LPC 16:0+Na]$^+$	-0.2

Supplementary Fig. 9 MS/MS spectrum of m/z 520.3400 ([LPC 18:2+H]+)

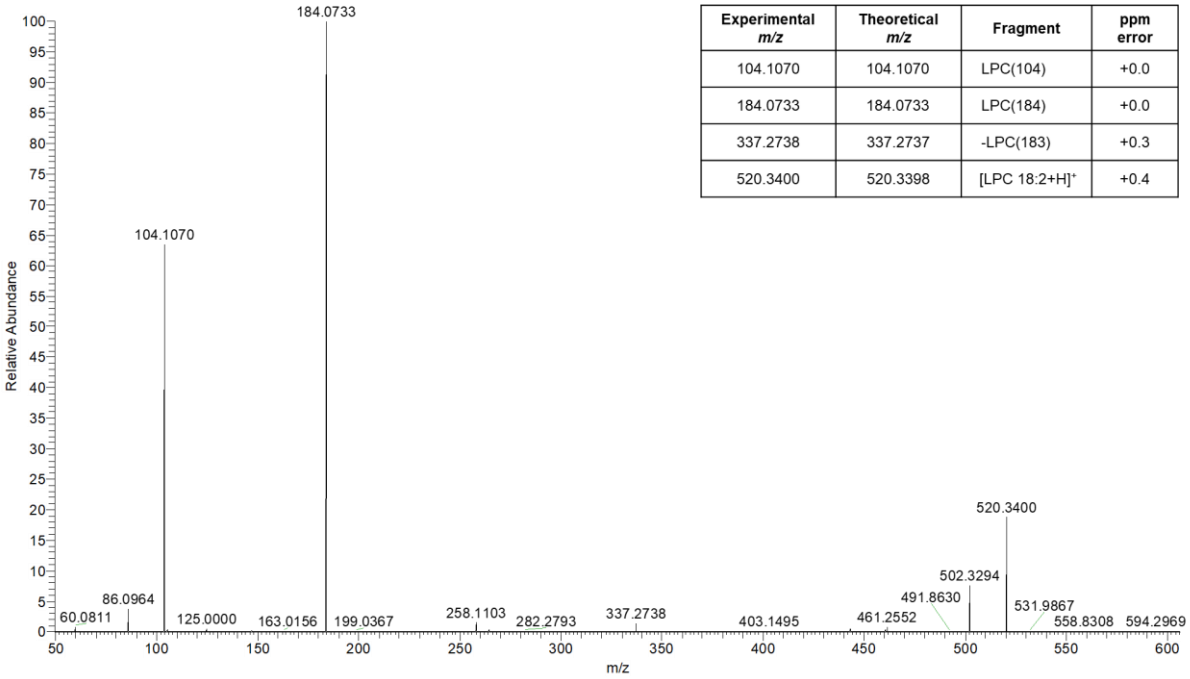

Experimental *m/z*	Theoretical *m/z*	Fragment	ppm error
104.1070	104.1070	LPC(104)	+0.0
184.0733	184.0733	LPC(184)	+0.0
337.2738	337.2737	-LPC(183)	+0.3
520.3400	520.3398	$[LPC\ 18:2+H]^+$	+0.4

Supplementary Fig. 10 MS/MS spectrum of m/z 522.3557 ([LPC 18:1+H]+)

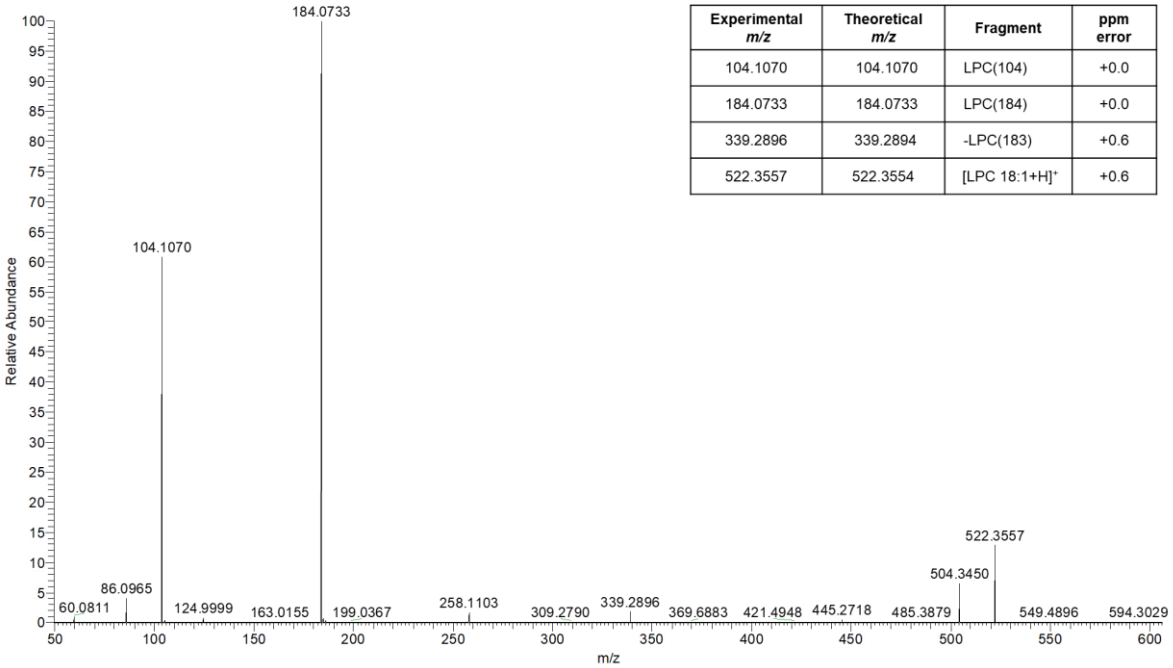

Experimental *m/z*	Theoretical *m/z*	Fragment	ppm error
104.1070	104.1070	LPC(104)	+0.0
184.0733	184.0733	LPC(184)	+0.0
339.2896	339.2894	-LPC(183)	+0.6
522.3557	522.3554	$[LPC\ 18:1+H]^+$	+0.6

Supplementary Fig. 11 MS/MS spectrum of m/z 524.3717 ([LPC 18:0+H]+)

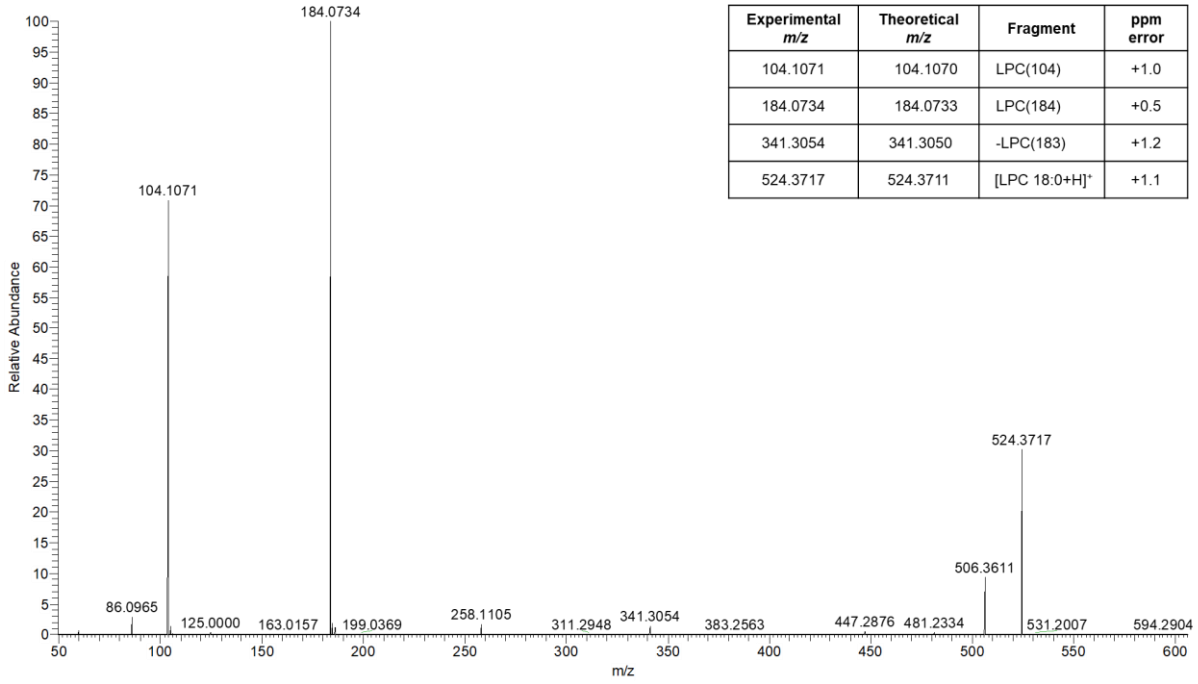

Experimental *m/z*	Theoretical *m/z*	Fragment	ppm error
104.1071	104.1070	LPC(104)	+1.0
184.0734	184.0733	LPC(184)	+0.5
341.3054	341.3050	-LPC(183)	+1.2
524.3717	524.3711	$[LPC\ 18:0+H]^+$	+1.1

Supplementary Fig. 12 MS/MS spectrum of m/z 534.2951 ([LPC 16:0+K]+)

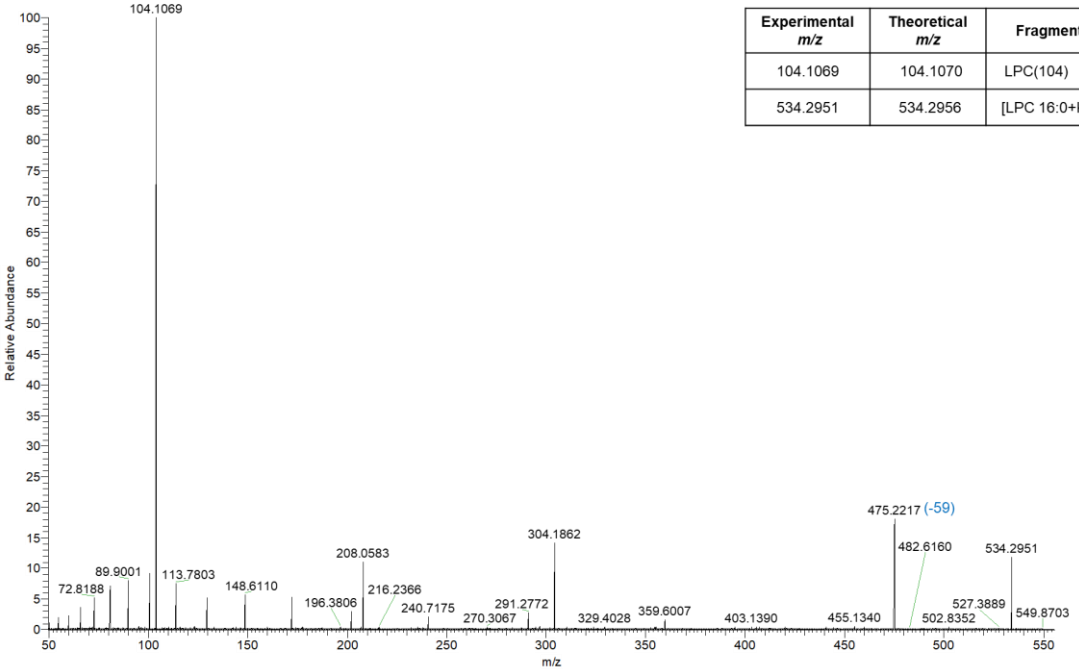

Experimental *m/z*	Theoretical *m/z*	Fragment	ppm error
104.1069	104.1070	LPC(104)	-1.0
534.2951	534.2956	[LPC 16:0+K]$^+$	-0.9

Supplementary Fig. 13 MS/MS spectrum of m/z 544.3389 ([LPC 18:1+Na]+)

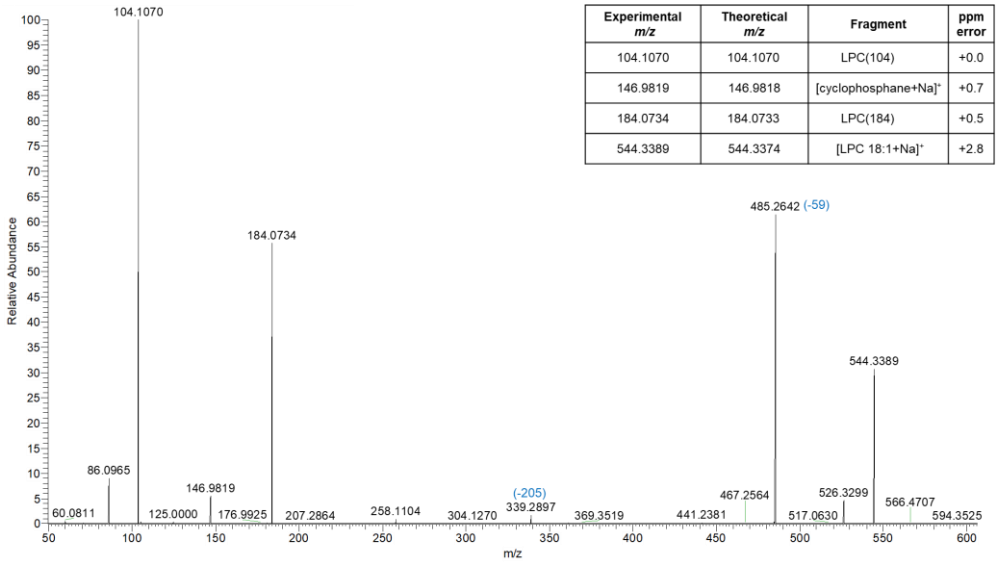

Experimental *m/z*	Theoretical *m/z*	Fragment	ppm error
104.1070	104.1070	LPC(104)	+0.0
146.9819	146.9818	[cyclophosphane+Na]$^+$	+0.7
184.0734	184.0733	LPC(184)	+0.5
544.3389	544.3374	[LPC 18:1+Na]$^+$	+2.8

Supplementary Fig. 14 MS/MS spectrum of m/z 546.3540 ([LPC 18:0+Na]+)

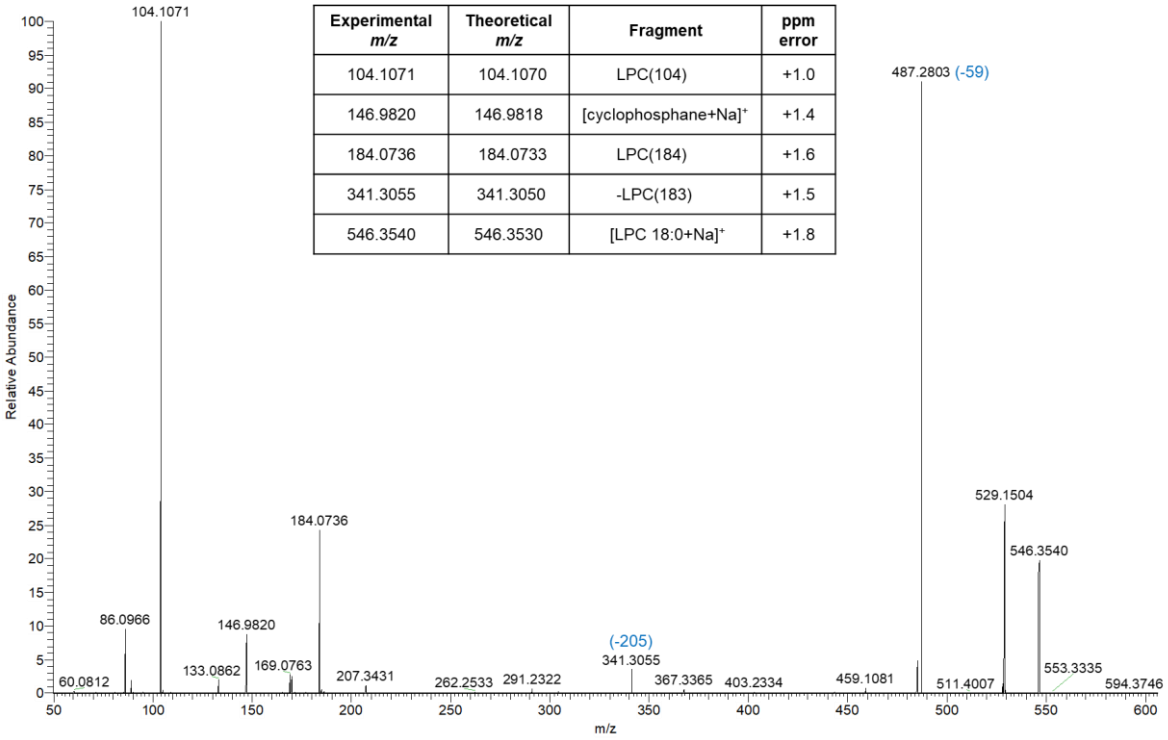

Experimental *m/z*	Theoretical *m/z*	Fragment	ppm error
104.1071	104.1070	LPC(104)	+1.0
146.9820	146.9818	[cyclophosphane+Na]$^+$	+1.4
184.0736	184.0733	LPC(184)	+1.6
341.3055	341.3050	-LPC(183)	+1.5
546.3540	546.3530	[LPC 18:0+Na]$^+$	+1.8

Supplementary Fig. 15 MS/MS spectrum of m/z 560.3123 ([LPC 18:1+K]+)

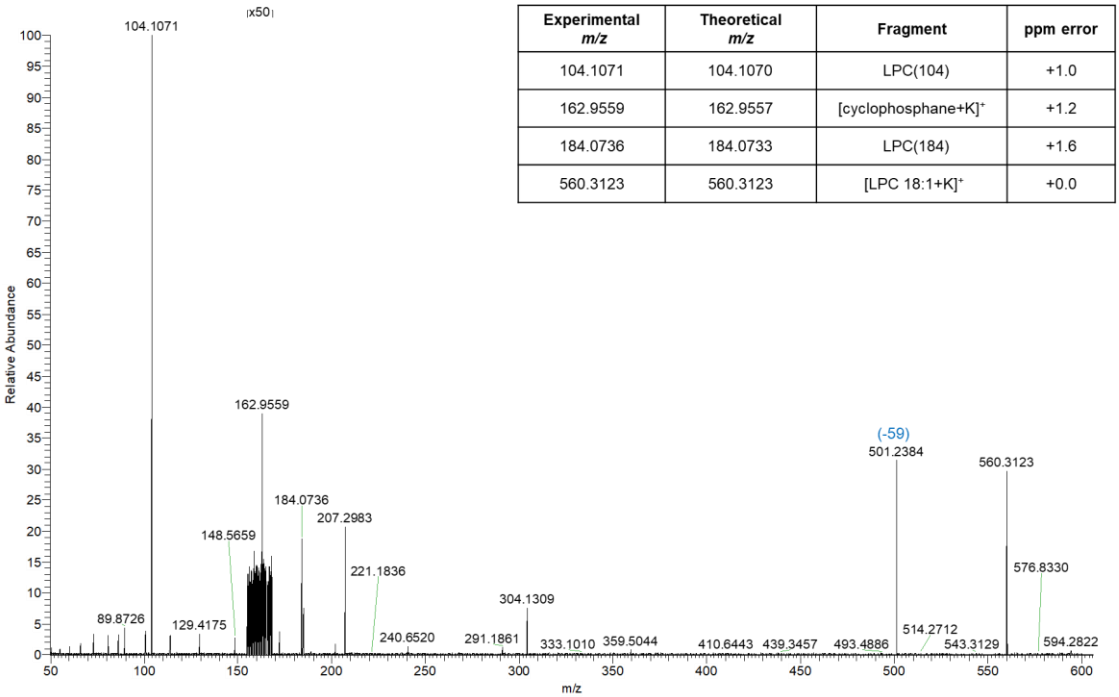

Experimental *m/z*	Theoretical *m/z*	Fragment	ppm error
104.1071	104.1070	LPC(104)	+1.0
162.9559	162.9557	[cyclophosphane+K]$^+$	+1.2
184.0736	184.0733	LPC(184)	+1.6
560.3123	560.3123	[LPC 18:1+K]$^+$	+0.0

Supplementary Fig. 16 MS/MS spectrum of m/z 562.3278 ([LPC 18:0+K]+)

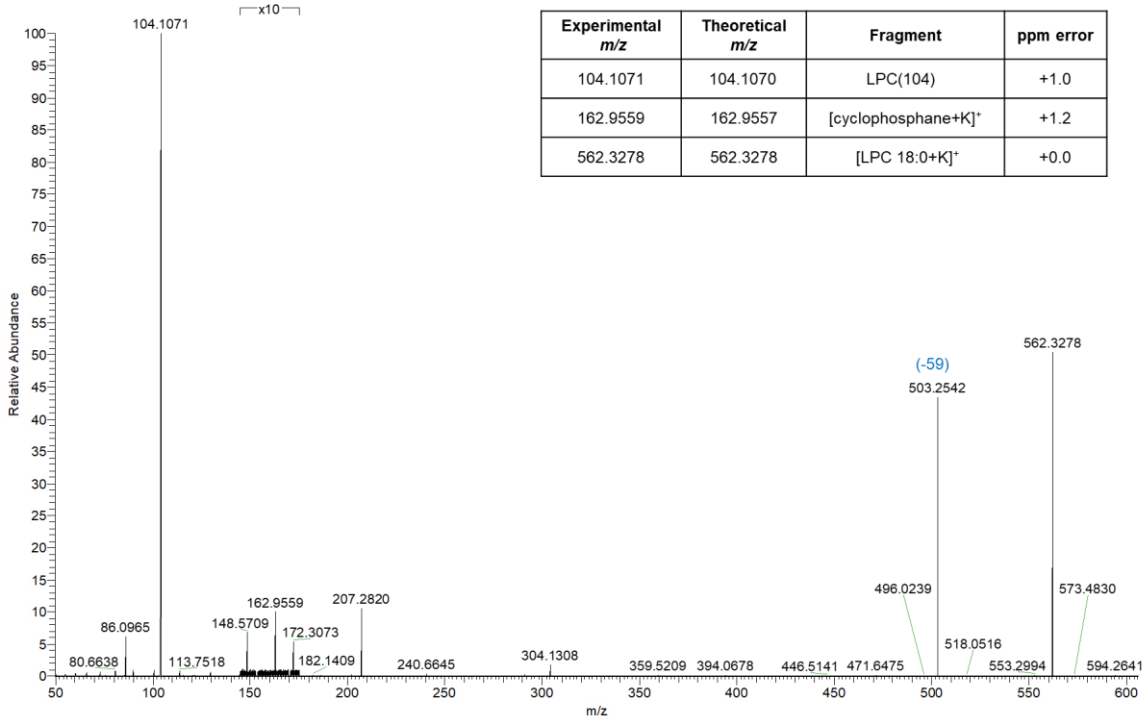

Experimental *m/z*	Theoretical *m/z*	Fragment	ppm error
104.1071	104.1070	LPC(104)	+1.0
162.9559	162.9557	[cyclophosphane+K]$^+$	+1.2
562.3278	562.3278	[LPC 18:0+K]$^+$	+0.0

Supplementary Fig. 17 MS/MS spectrum of m/z 599.3216 ([LPI 18:0-H]$^-$)

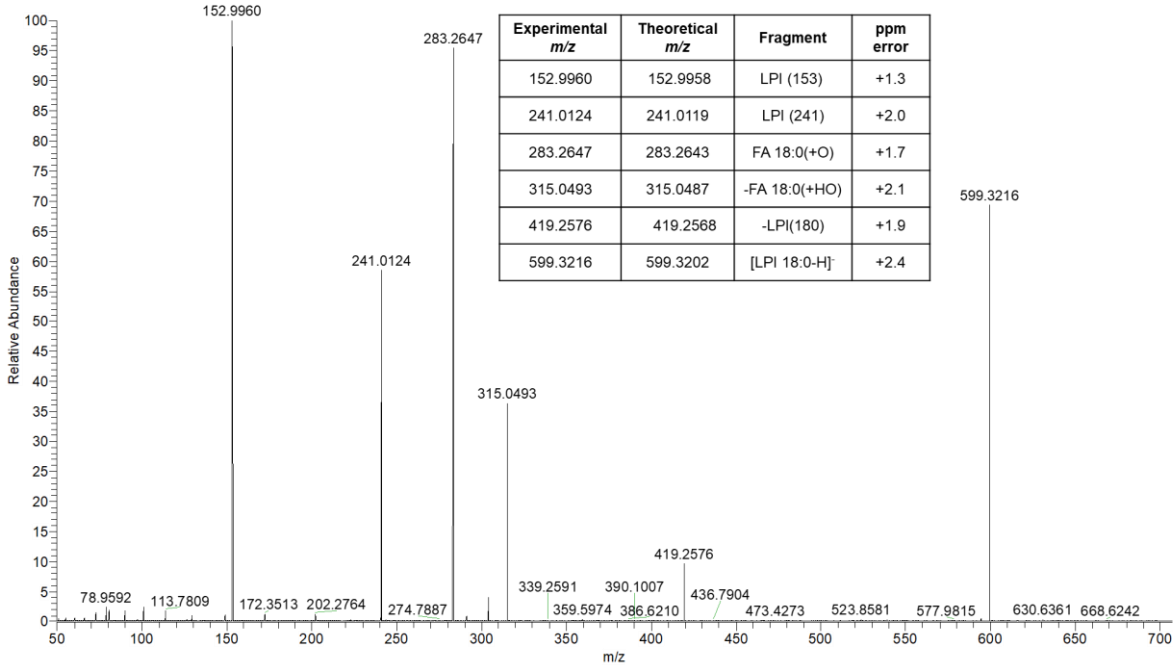

Experimental *m/z*	Theoretical *m/z*	Fragment	ppm error
152.9960	152.9958	LPI (153)	+1.3
241.0124	241.0119	LPI (241)	+2.0
283.2647	283.2643	FA 18:0(+O)	+1.7
315.0493	315.0487	-FA 18:0(+HO)	+2.1
419.2576	419.2568	-LPI(180)	+1.9
599.3216	599.3202	[LPI 18:0-H]$^-$	+2.4

Supplementary Fig. 18 MS/MS spectrum of m/z 619.2895 ([LPI 20:4-H]$^-$)

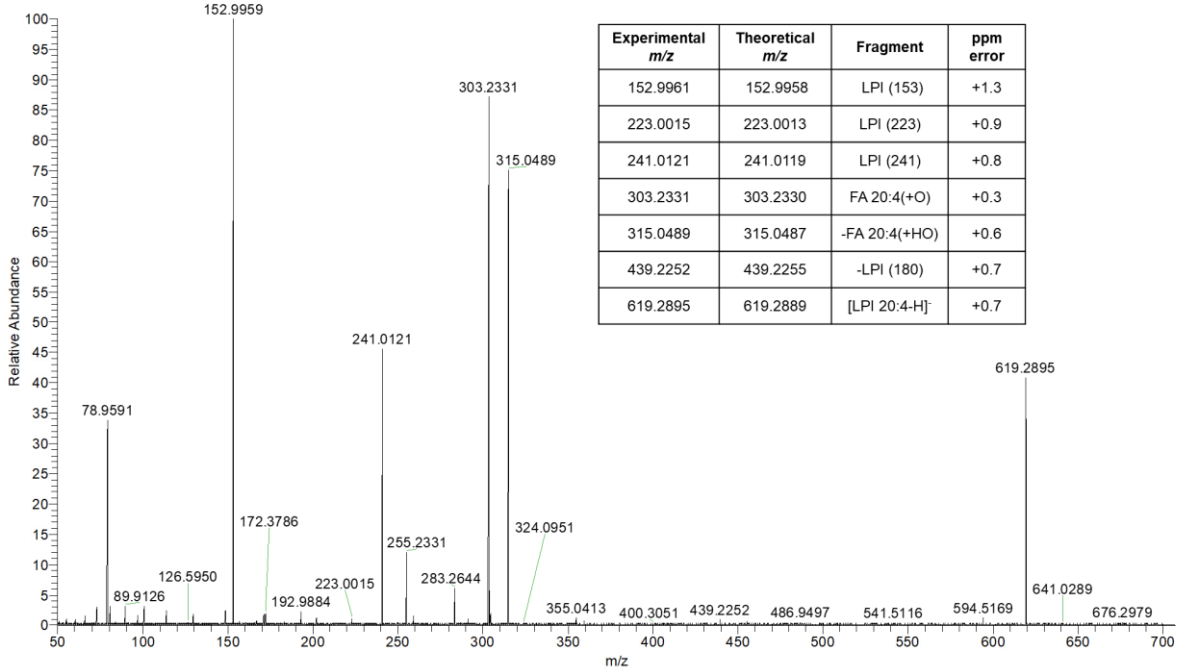

Experimental *m/z*	Theoretical *m/z*	Fragment	ppm error
152.9961	152.9958	LPI (153)	+1.3
223.0015	223.0013	LPI (223)	+0.9
241.0121	241.0119	LPI (241)	+0.8
303.2331	303.2330	FA 20:4(+O)	+0.3
315.0489	315.0487	-FA 20:4(+HO)	+0.6
439.2252	439.2255	-LPI (180)	+0.7
619.2895	619.2889	[LPI 20:4-H]$^-$	+0.7

Supplementary Fig. 19 MS/MS spectrum of m/z 687.5462 ([SM d18:1_16:0-CH_3]$^-$)

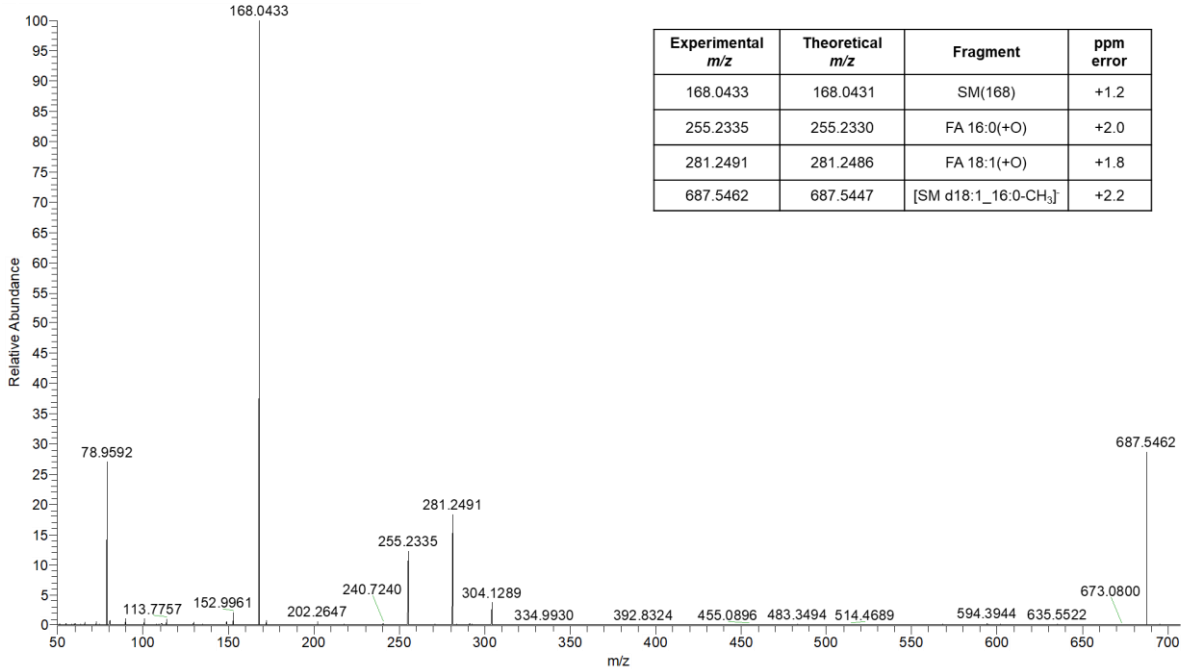

Experimental *m/z*	Theoretical *m/z*	Fragment	ppm error
168.0433	168.0431	SM(168)	+1.2
255.2335	255.2330	FA 16:0(+O)	+2.0
281.2491	281.2486	FA 18:1(+O)	+1.8
687.5462	687.5447	[SM d18:1_16:0-CH_3]$^-$	+2.2

Supplementary Fig. 20 MS/MS spectrum of m/z 689.5620 ([SM d18:0_16:0-CH_3]$^-$)

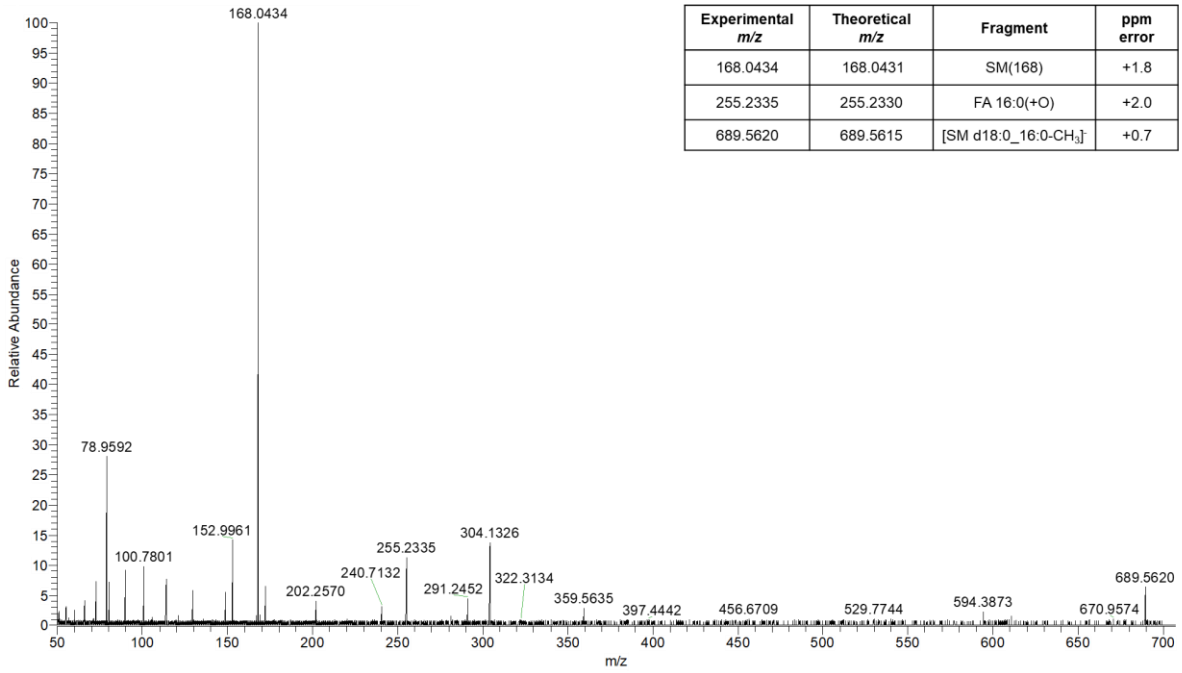

Experimental *m/z*	Theoretical *m/z*	Fragment	ppm error
168.0434	168.0431	SM(168)	+1.8
255.2335	255.2330	FA 16:0(+O)	+2.0
689.5620	689.5615	[SM d18:0_16:0-CH_3]$^-$	+0.7

Supplementary Fig. 21 MS/MS spectrum of m/z 725.5583 ([SM 34:1;2+Na]$^{+}$)

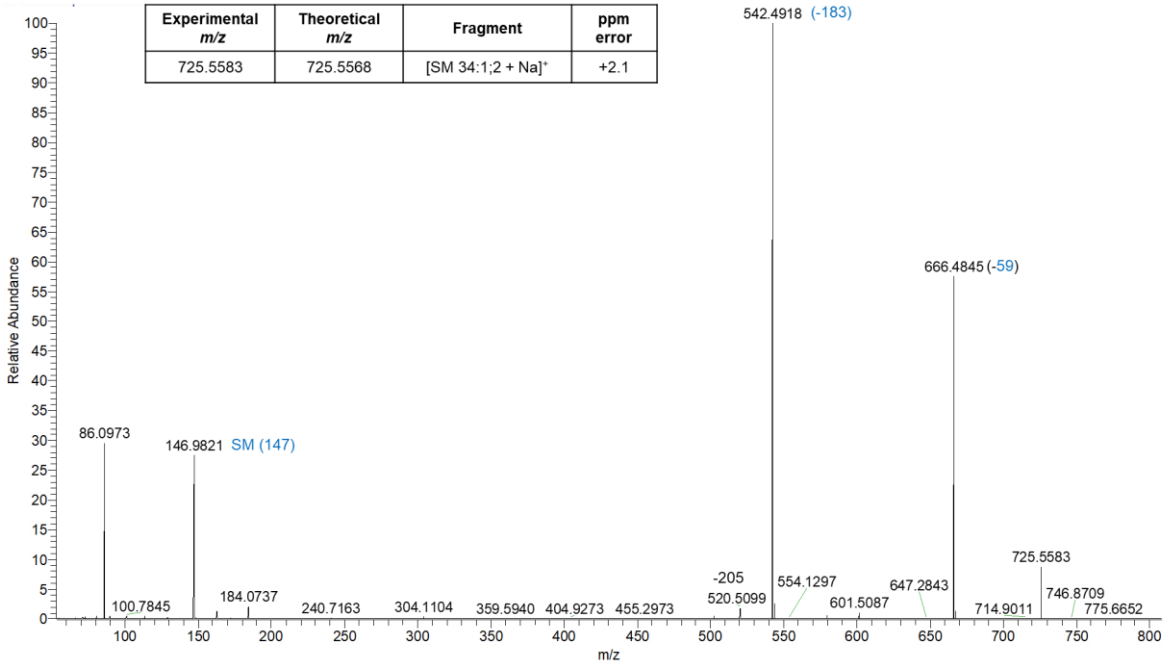

Supplementary Fig. 22 MS/MS spectrum of m/z 727.5731 ([SM 34:0;2+Na]$^{+}$)

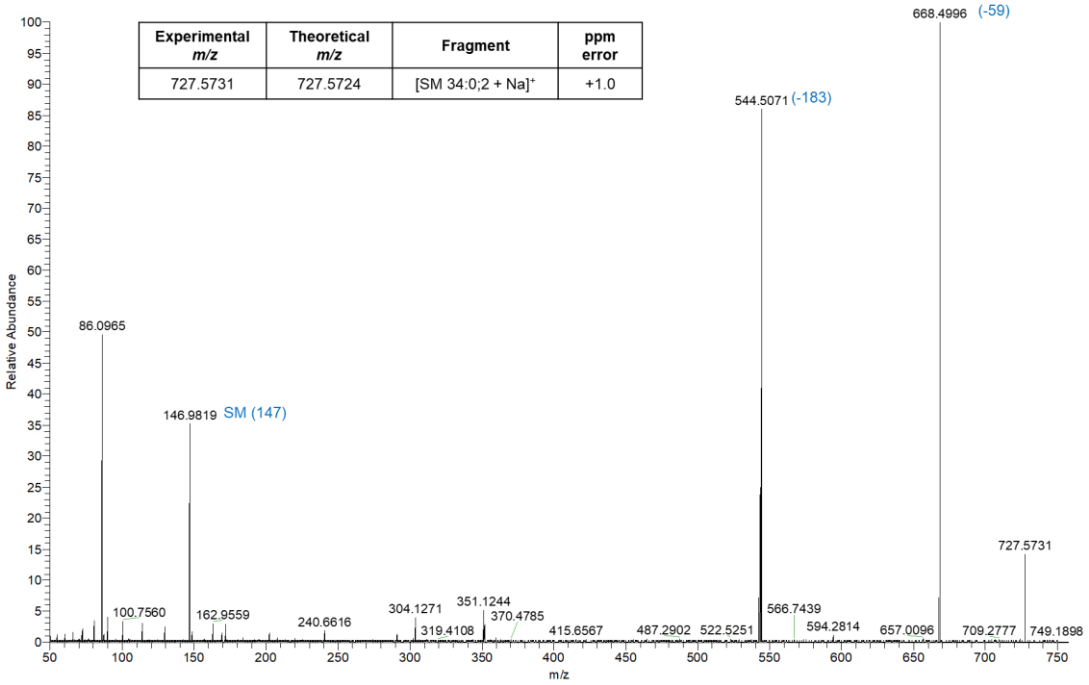

Supplementary Fig. 23 Spatial correlation of all identified m/z species to the plaque area on a section-by-section basis in the 3D MSI experiment

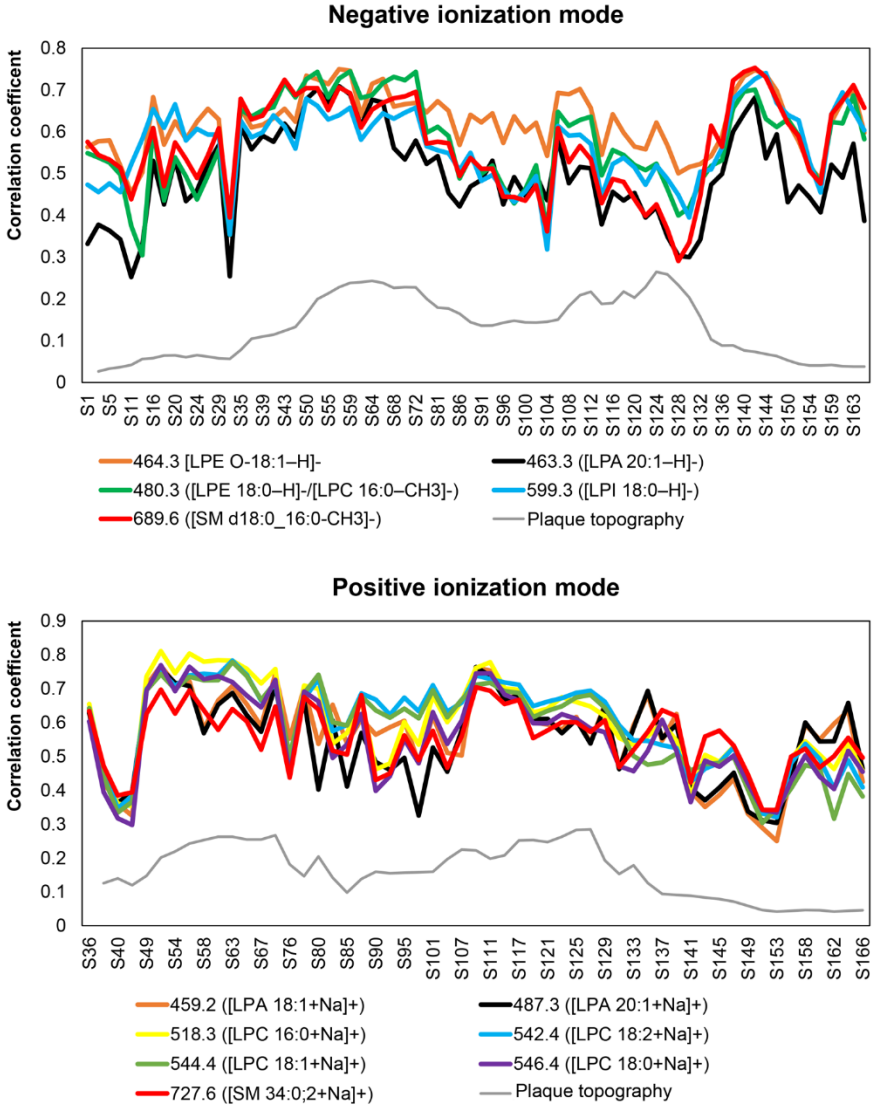

Supplementary Fig. 24 Spatial distribution of several cholesteryl esters.

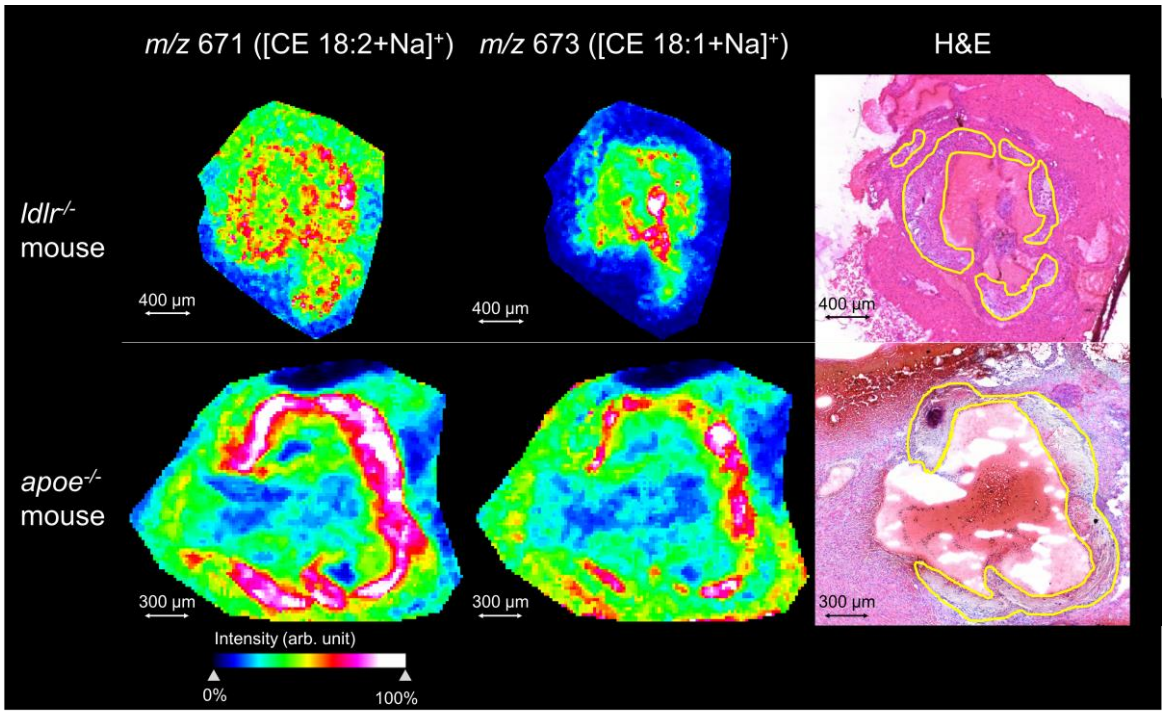

Supplementary Fig. 25 Spatial distribution of several oxysterols.

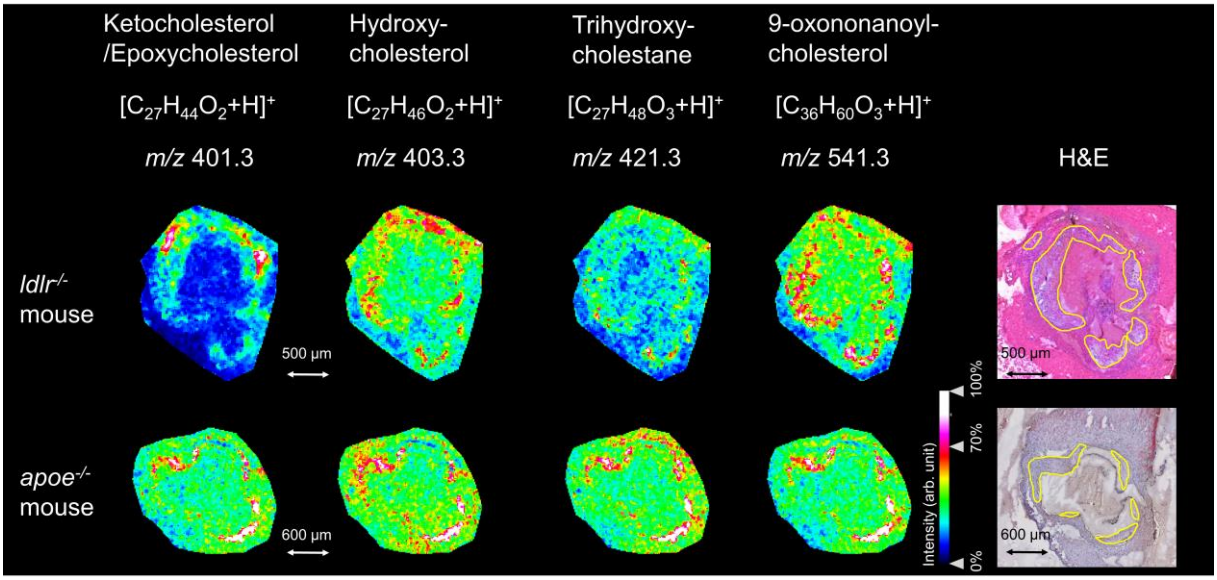

Supplementary Fig 26 Sphingomyelin 34:0 is detected in both ionization modes.